Article

Ceria doped Zinc Oxide Nanoflowers Enhanced Luminol-based Electrochemiluminescence Immunosensor for Amyloid-# Detection

Jingxi Wang, Ying Zhuo, Ying Zhou, Haijun Wang, Ruo Yuan, and Yaqin Chai

ACS Appl. Mater. Interfaces, **Just Accepted Manuscript** • DOI: 10.1021/acsami.6b00021 • Publication Date (Web): 05 May 2016

Ceria doped Zinc Oxide Nanoflowers Enhanced Luminol-based Electrochemiluminescence Immunosensor for Amyloid-β Detection

Jing-Xi Wang, Ying Zhuo, Ying Zhou, Hai-Jun Wang, Ruo Yuan, Ya-Qin Chai**

Key Laboratory of Luminescent and Real-Time Analytical Chemistry (Southwest University), Ministry of Education, College of Chemistry and Chemical Engineering, Southwest University, Chongqing 400715, PR China

*Corresponding authors at: Tel.: +86 23 68252277, fax: +86 23 68253172.

E-mail addresses: yuanruo@swu.edu.cn (R. Yuan); yqchai@swu.edu.cn (Y.Q. Chai).

ABSTRACT: In this work, a ceria doped ZnO nanomaterial with flower-structure (Ce:ZONFs) was prepared to construct a luminol-based electrochemiluminiscence (ECL) immunosensor for amyloid-β protein (Aβ) detection. Herein, carboxyl groups (-COOH) covered Ce:ZONFs were synthesized by a green method with lysine as reductant. After that, Ce:ZONFs based ECL nanocomposite was prepared by combining the luminophore of luminol and Ce:ZONFs via amidation and physical absorption. Luminol modified on Ce:ZONFs surface could generate a strong ECL signal under the assistance of reactive oxygen species (ROSs) (such as $OH^{\cdot}$ and $O_2^{\cdot-}$), which were produced by a catalytic reaction between Ce:ZONFs and H_2O_2. It was worth noticing that a quick $Ce^{4+} \leftrightarrow Ce^{3+}$ reaction in this doped material could increase the rate of electron transfer to realize the signal amplification. Subsequently, the luminol functionalized Ce:ZONFs (Ce:ZONFs-Lum) were covered by secondary antibody (Ab_2) and glucose oxidase (GOD), respectively, to construct a novel Ab_2 bioconjugate (Ab_2-GOD@Ce:ZONFs-Lum). The wire-structured silver-cysteine complex (AgCys NWs) with a large number of -COOH, which was synthesized by $AgNO_3$ and L-cysteine, was used as substrate of the immunosensor to capture the primary antibody (Ab_1). Under the optimal conditions, this proposed ECL immunosensor had exhibited high sensitivity for Aβ detection with a wide linear range from 80 fg/mL to 100 ng/mL and an ultralow detection limit of 52 fg/mL. Meanwhile, this biosensor had good specificity for Aβ, indicating that the provided strategy had a promising potential in the detection of Aβ.

KEYWORDS: Electrochemiluminescence, immunosensor, ceria doped zinc oxide nanoflowers, luminol, amyloid-β

1. Introduction

Alzheimer's disease (AD), a very common form of late-life dementia, has been considered as a worldwide health problem. The main characteristic symptoms of AD include necrosis of part of neurons, gradual memory loss and abnormal formation of neurotic in cerebrum[1,2]. Based on the AD research, amyloid-β protein (Aβ) was proved to be the pathogenesis of AD due to its extremely strong neurotoxicity[3,4]. Thus, Aβ can be used as one of the main AD-related specific biomarkers in AD detection, presenting a positive and practical significance for early prevention and treatment for AD.

ECL immunosensor is an ECL immune-modified sensing platform with the advantages of better specificity, higher sensitivity, etc[5], which has been widely used to detect disease markers via immune-reaction[6,7,8], the ECL signal can be used as characteristic signal for real-time monitoring the level of disease marker. To the best of our knowledge, luminol is one of the most commonly used luminophore in ECL system because of its high emitting efficiency and low cost[9,10]. Considering these advantages of luminol, a luminol-based ECL immunosensor had been constructed for Aβ detection in this work.

ZnO-based nanomaterial is a superior nano-catalyst[11,12] and the introduction of rare earth elements into ZnO can effectively improve its catalytic activity[13,14]. Ceria (CeO_2), an oxide of rare earth element, has received great attention for its unique catalytic properties in redox reactions[15,16,17]. Moreover, the redox pair Ce^{3+}/Ce^{4+} of CeO_2 could switch reversibly and rapidly[18,19], which endowed high catalytic activity and electron transfer rate. Thus, with the help of lysine, the ceria doped ZnO nanoparticles (Ce:ZONPs) with full of carboxyl groups (-COOH) and amino groups ($-NH_2$) had been successfully developed[20,21,22] to increase the property of luminol-based ECL immunosensor. This hybrid material acted as an enzyme-mimic, which exhibits an excellent electrocatalytic performance in H_2O_2 decomposition to produce reactive oxygen species (ROSs) including $OH^{\cdot}$ and $O_2^{\cdot-}$[23], promoting the ECL efficiency of luminol to get a strong ECL signal. Moreover, a much stronger ECL signal of luminol can be obtained because of the quick $Ce^{4+}\leftrightarrow Ce^{3+}$ reaction. It is worth stressing that when compared with nature enzymes such as horse radish peroxidase (HRP), the nanostructured enzyme mimics could overcome the drawbacks of nature enzymes in enviromental and thermal instability[24,25].

Herein, a versatile ECL immunosensor based on ceria doped ZnO nanoflowers (Ce:ZONFs) was developed for the detection of Aβ. The luminophore of luminol was bound to Ce:ZONFs surface via amidation and physical adsorption, obtaining a nanocomposite of Ce:ZONFs-Lum to act as a signal probe. Then, H_2O_2 generated in situ via a catalytic reaction between glucose and glucose oxidase (GOD) and further

catalyzed by Ce:ZONFs to produce ROSs, which promoted the emission of luminol. And the fast $Ce^{4+}\leftrightarrow Ce^{3+}$ shift could increase the electron transfer rate and further enhance the ECL emission effectively. Meanwhile, a protein-like silver-cysteine nanowire (AgCys NWs) with superior biocompatibility was synthesized[26]. The ECL immunosensing platform was created by immobilizing primary antibody (Ab_1) on AgCys NWs decorated glassy carbon electrode (GCE). Consequently, a sandwiched ECL immunosensor was proposed for Aβ detection with high sensitivity and specificity.

2. Experimental

2.1 Chemicals and apparatus

Luminol (98%), Bovine serum albumin (BSA, 96%-98%) and Glucose oxidase (GOD) had been bought from Sigma-Aldrich Co. (St. Louis, MO, USA). Cerium (III) nitrate hexahydrate ($Ce(NO_3)_3\cdot 6H_2O$), zinc nitrate hexahydrate ($Zn(NO_3)_2\cdot 6H_2O$) and sodium hydroxide (NaOH) were acquired from Chengdu Kelong Chemical Industry (Chengdu, China). Gold chloride tetrahydrate ($HAuCl_4\cdot 4H_2O$) was purchased from Shanghai Fine Chemical Materials Institute (Shanghai, China). Silver nitrate ($AgNO_3$) was get from Sinopharm Chemical Reagent Co., Ltd (Shanghai, China). 1-(3-Dimethylaminopropyl)-3-ethylcarbodiimide hydrochloride (EDC) and N-hydroxy succinimide (NHS) were supplied by Shanghai Medpep Co. (Shanghai,

China). Lysine and Cysteine were supplied by J&K Scientific (Beijing, China). Amyloid-β protein (Aβ) and its antibody were both obtained from Shanghai Xin Yu Biotech Co., Ltd (Shanghai, China). α-1-fetoprotein (AFP), carcinoembryonic antigen (CEA) and their relative antibodies were provided by Biocell Company (Zhengzhou, China). The luminol solution (25 mM) in this research was prepared by dissolving the luminol powder in NaOH solution (0.1 M) and then kept in the refrigerator for further usage. The Phosphated buffered solution (PBS, 0.1 M, pH 7.4) with 0.1 M KCl, 0.1 M Na_2HPO_4, and 0.1 M KH_2PO_4 was used as dispersion and detection buffer in this research. In addition, the deionized water (18.2 $M\Omega \cdot cm^{-1}$) was employed in this research.

All electrochemical behaviors including cyclic voltammetric (CV), electrochemical impedance spectroscopy (EIS) and gold electrodeposition were implemented by a CHI 660C Electrochemistry Workstation (Shanghai CH Instruments, China). The ECL emission was tested by a MPI-E Electrochemiluminescence Analyzer (Xi'an Remax Electronic High-Tech Ltd, China). In the process of ECL testing, the voltage of the photomultiplier tube (PMT) was set at 800 V and the scanning potential was from 0.2 V to 0.8 V. And a three-electrode system including a Pt wire served as counter electrode, a GCE (Φ = 4 mm) used as working electrode and Ag/AgCl (*sat.* KCl) acted as reference electrode had been used throughout the ECL detection. The morphologies and the composition of different nanoparticles had been characterized by Scan electron

microscope (SEM, S-4800, Hitachi, Japan) and X-ray Photoelectron spectroscopy (XPS, Thermoelectricity Instruments, USA). The UV-vis spectra of these nanomaterials were carried out with a UV-vis spectrophotometer (UV-2450, Shimadzu, Japan).

2.2 Synthesis of AgCys NWs

AgCys NWs were prepared according to the method reported previously with a minor modification[26]. 2 mL cysteine solution (75 mM) was added into 5 mL $AgNO_3$ solution (25 mM) with a slow stirring for 30 min, and then ripened at 50°C for 1 h to obtain the white sediment. Then this sediment was centrifugated and washed by deionized water to obtain AgCys NWs. And the synthesized AgCys NWs was kept at cold and dark place when not be used.

2.3 Preparation of Ce:ZONFs

The ceria doped ZnO nanoflowers (Ce:ZONFs) were synthesized according to the method reported previously with a minor modification[20,21,22]. Firstly, 10 mL $Zn(NO_3)_2$ solution (6 mM) and 500 μL $Ce(NO_3)_3$ (2 mM) were mingled with 1 mL cysteine (0.1 M) with a stirring for 2 h at 80°C. Then 5 mL lysine (0.1 M) had been added into the mixture for another 5 min stirring. After that, this mixed solution had been transferred into an autoclave and kept heating at 180°C for 12 h to generate Ce:ZONFs. After the process of centrifugation, pure Ce:ZONFs could be obtained.

Finally, the Ce:ZONFs were redispersed in deionized water and stored at room temperature for further usage.

2.4 Preparation of Ab_2 bioconjugate (Ab_2-GOD@Ce:ZONFs-Lum)

The preparation process of Ab_2-GOD@Ce:ZONFs-Lum bioconjugate was showed in Scheme 1(A). Firstly, in order to activate the carboxyl of Ce:ZONFs surface, 2 mL Ce:ZONFs dispersion liquid mixed with EDC (40 mM) and NHS (10 mM) for 30 min at 4°C. Then 200 μL luminol (25 mM) was dropped into the mixture with a stirring for another 4 h to bind luminol on the surface of Ce:ZONFs via amide reaction. In the same way, 200 μL anti-Aβ (Ab_2) could be immobilized on the surface of Ce:ZONFs after 12 h stirring at 4°C. Afterwards, 100 μL of GOD (5%) served as blockers was added into above mixture to prevent nonspecific adsorption. After centrifugation and washing for several times, the bioconjugate (Ab_2-GOD@Ce:ZONFs-Lum) was prepared and dispersed in 1 mL of PBS buffer (0.1 M).

2.5 Fabrication of ECL immunosensor

The fabrication process of ECL immunosensor was shown in Scheme 1. Firstly, GCE was pretreated by 0.3 μm and 0.05 μm of alumina slurries to get a mirror-like surface, and then it was washed with deionized water, alcohol, and deionized water respectively. Subsequently, the GCE was immersed into $HAuCl_4$ (1%) to electrodeposit a layer of AuNPs (DpAu) at a constant potential of -0.2 V for 30 s.

Then, 10 μL of prepared AgCys NWs was covered on the DpAu modified GCE and dried in the air to form film. After that, 10 μL Ab_1 was coated on the surface of AgCys/DpAu/GCE for 12 h at 4°C. Lastly, 10 μL BSA (1%) was dropped onto the electrode to block the remaining nonspecific binding sites of the immunosensor. Then the prepared immunosensor was kept in 4°C for the following experiment.

2.6 ECL measurement

First of all, the proposed immunosensor was washed thoroughly with PBS buffer, and then incubated with Aβ antigen for 40 min at 37°C. Subsequently, 10 μL of Ab_2 bioconjugate was incubated on the immunosensor for another 40 min at room temperature to construct a sandwiched format to detect Aβ antigen. Lastly, the ECL signal was tested in 2 mL PBS buffer with 10 mM glucose. With the increasing of Aβ antigen concentration, more Ab_2 bioconjugate could be immobilized on the immunosensor, which may result in a stronger ECL signal. According to the changes of ECL intensity, Aβ antigen could be detected quantitatively.

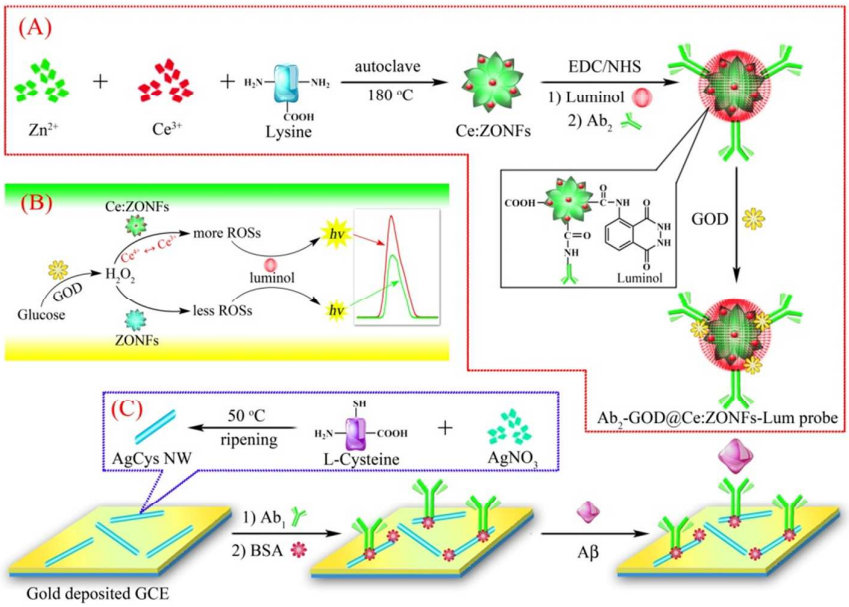

Scheme 1 Schematic illustration of (A) Synthesis process of Ab_2-GOD@Ce:ZONFs-Lum signal probe; (B) Possible ECL mechanism of signal generation and enhancement; and (C) Preparation process of the AgCys nanowires.

3. Results and discussions

3.1 Characterizations of nanomaterials

As illustrated in Fig. 1A, the pure ZnO nanoflowers (ZONFs) with a smooth surface and an average partical size of 400 nm could be observed clearly. Compared with pure ZONFs, the ceria doped ZONFs presented a lotus-like structure with more "petals" and their surface was quite rough (shown in Fig. 1B). When Ce:ZONFs were combined with luminol via EDC/NHS, the morphology of Ce:ZONFs-Lum exhibited a great difference to ZONFs or Ce:ZONFs, which had a olive-like structure with more rough surfaces and larger specific surface areas (shown in Fig.

1C). This difference might be attributed to the activated carboxyl group which further enhanced the hydrophilicity of Ce:ZONFs and caused the greatly morphology changing.

Simultaneously, the SEM image of AgCys NWs was showed in Fig. S1 (Supporting Information), a nanowire structured AgCys complex could be observed clearly, and the average length and diameter of which were 2.5 μm and 250 nm, respectively. In order to further study the properties of AgCys NWs, the FT-IR and UV-vis spectra of AgCys had been characterized and the results were showed in Fig. S2 (Supporting Information). As shown in Fig. S2(a), two strong IR peaks were obtained at 1585.49 cm^{-1} and 1386.34 cm^{-1}, illustrating the existence of $–COO^-$, which demonstrated the ionization of –COOH. And a characteristic absorption peak of cysteine at 2553cm^{-1} (S-H) was disappeared, indicating S-H was replaced by Ag-S in AgCys nanowire. Fig. S2(b) was the UV-vis spectrum of AgCys NWs, the absorption peak at 210 nm could further demonstrated the existence of –COOH.

In order to confirm the elements of Ce:ZONFs-Lum, an XPS characterization had been presented in Fig. 1D. Clearly seen from Fig. 1D(a), all characteristic peaks of Zn2p, Ce3d, O1s, N1s and C1s were present in Ce:ZONFs-Lum. Meanwhile, Fig. 1D(b) and (c) exhibited the XPS spectra of zinc ion and cerium ion, respectively. The peaks at 1022.07 eV ($Zn2p_{3/2}$) and 1045.08 eV ($Zn2p_{1/2}$) represented the existence of ZnO and the XPS peak at 886.2 eV confirmed the presence of cerium.

These results confirmed the successful preparation of Ce:ZONFs-Lum and AgCys NWs.

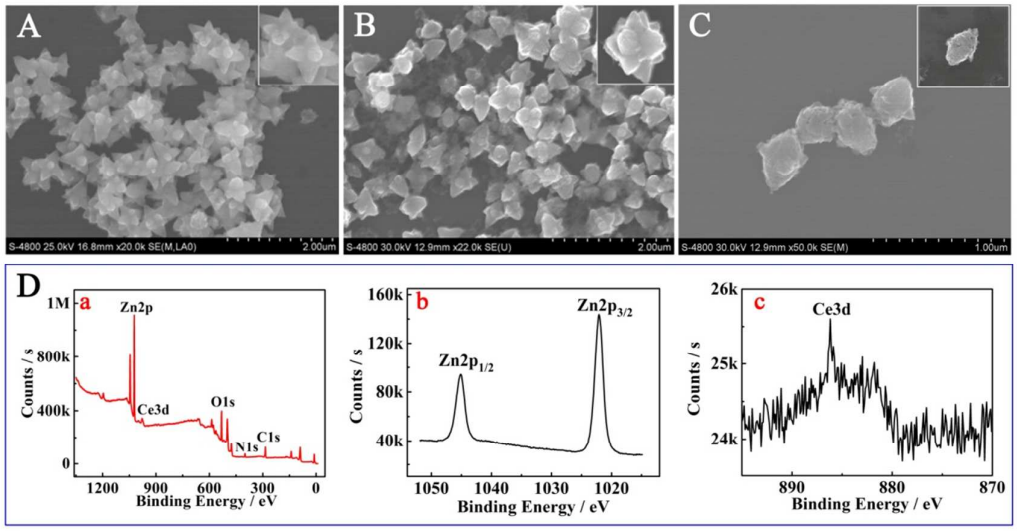

Fig. 1 SEM images of (A) pure ZONFs, (B) Ce:ZONFs, and (C) Ce:ZONFs-Lum; The insets of (A), (B) and (C) were the partly enlarged images of the relative nanomaterials. (D) XPS spectra of (a) the full region for Ce:ZONFs-Lum, (b) Zn2p region and (c) Ce3d region.

3.2 Characterizations of the proposed ECL immunosensor

CV characterizations of each step in the construction of immunosensor were performed in 0.1 M PBS including 5.0 mM $[Fe(CN)_6]^{3-/4-}$. Fig. 2A showed that the bare GCE had a well-defined redox peak in $[Fe(CN)_6]^{3-/4-}$ solution (curve a). After DpAu was modified on bare GCE, an apparently increased peak current (curve b) was obtained for the superior conductivity of DpAu. Then AgCys NRs were covered on DpAu/GCE, the redox wave decreased a bit (curve c) because the AgCys

complex hindered the electron transfer. When Ab_1 was assembled on the electrode, the current was further reduced (curve d), owing to the insulated effect of protein. Followed that, the modified GCE was incubated with BSA (1%) and Aβ respectively (curve e, f), and the redox currents declined successively for the non-conductivity of proteins.

Meanwhile, the EIS characteristics were represented in Fig. 2B, the electron-transfer resistance of DpAu/GCE (curve b) was much smaller than that of the bare GCE (curve a), this was because DpAu had superior conductivity. As AgCys had been dropped onto DpAu/GCE, the resistance was increased (curve c). After that, the primary antibody, BSA and antigen were added on GCE, respectively. The electron-transfer resistance was further increased (curve d, e, f). Therefore, both the CV and EIS results indicated that the immunosensor was successfully fabricated.

In order to prove that luminol was immobilized on Ab_2 bioconjugate and the sandwich-type ECL immunosensor was available for Aβ detection, the ECL behavior of the immunosensor had been detected in PBS with 10 mM glucose. From Fig. 2C, when Ab_2-GOD@Ce:ZONFs bioconjugate was bound with Aβ antigen, no ECL signal had been observed (blue curve) for the absence of luminol. On the contrary, after the prepared Ab_2 bioconjuate (Ab_2-GOD@Ce:ZONFs-Lum) was decorated on the immunosensor surface, an extremely strong ECL signal (red curve) could be detected, indicated that luminol could generate strong ECL emission and it had been immobilized on Ab_2 bioconjugate. In addition, an ECL spectrum of the

luminol functionalized Ab_2 bioconjugate was presented in Fig. S3 (Supporting Information), and the maximum wavelength of the bioconjugate was 420 nm.

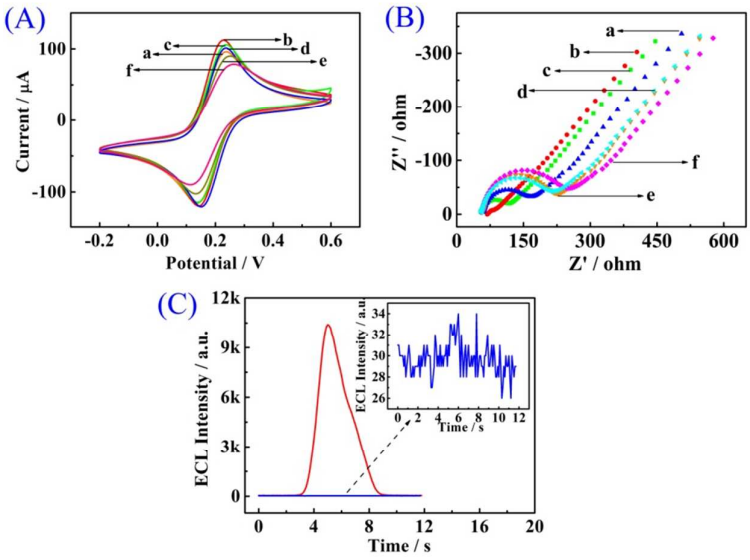

Fig. 2 (A) CVs for each fabricated step in PBS containing 5 mM $[Fe(CN)_6]^{3-/4-}$: (a) Bare GCE, (b) DpAu/GCE, (c) AgCys/DpAu/GCE, (d) Ab_1/AgCys/DpAu/GCE, (e) BSA/Ab_1/AgCys/DpAu/GCE, and (f) Aβ/BSA/Ab_1/AgCys/DpAu/GCE. (B) EIS responses of (a) Bare GCE, (b) DpAu/GCE, (c) AgCys/DpAu/GCE, (d) Ab_1/AgCys/DpAu/GCE, (e) BSA/Ab_1/AgCys/DpAu/GCE, and (f) Aβ/Ab_1/AgCys/DpAu/GCE. (C) ECL responses of the immunosensor in 10 ng/mL Aβ when incubated with Ab_2-GOD@Ce:ZONFs bioconjugate (blue curve) and Ab_2-GOD@Ce:ZONFs-Lum bioconjugate (red curve), respectively.

3.3 Optimizations of the volume of luminol and incubation time of Ab_2 bioconjugate

An experiment of a volume optimization of luminol (25 mM) had been performed in 2 mL PBS including 10 mM glucose (pH 7.4)[27]. As shown in Fig. 3A, with

increasing the volume of luminol, the ECL intensity increased rapidly and tended to be stable at the volume of 200 μL. Thus the optimal volume of luminol was 200 μL at last.

Meanwhile, the incubation time of Ab_2 bioconjugate influenced the ECL intensity directly. As shown in Fig. 3B, at the time of 40 min, an optimal ECL intensity was obtained. Through the result of the experiment, it could be confirmed that the antigen and antibody could form a stable immuno-complex at 40 min, which had been made as the optimal Ab_2 incubation time in the follow experiments.

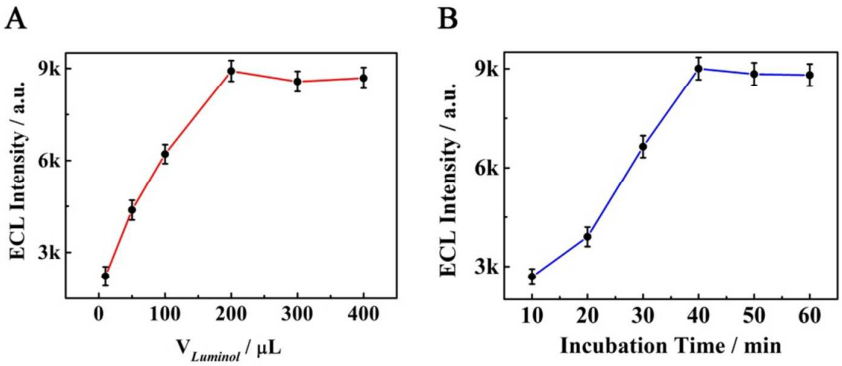

Fig. 3 Optimization of (A) the volume of luminol (25 mM), and (B) the incubation time of Ab_2 bioconjugate. All the ECL signals were detected in 2 mL PBS with 10 mM glucose (pH 7.4), and the concentration of Aβ was 10 ng/mL.

3.4 Comparison of ECL responses with different Ab_2 probes

A signal comparison of different Ab_2 probes was exhibited in Fig. 4A. Under the optimal conditions, two different Ab_2 probes were prepared to investigate the ECL amplification properties. They were the proposed ECL signal probe of

Ab_2-GOD@Ce:ZONFs-Lum (a) and the comparison probe of Ab_2-GOD@ ZONFs-Lum (b). Then the immunosensors were incubated with the same Aβ concentration of 10 ng/mL, and was further incubated with the preceding two different Ab_2 probes, respectively. As a result, as shown in Fig. 4A(a), a strong ECL signal (10401 a.u.) of the proposed ECL signal probe was obtained in PBS with 10 mM glucose. Simultaneously, a lower ECL signal (6818 a.u.) was obtained from the comparison probe in the same PBS buffer (Fig. 4A(b)).

The difference between (a) and (b) in Fig. 4A might contribute to the existence of Ce^{3+}/Ce^{4+} redox couple. The ceria doped ZnO could lose electrons to generate the electron-hole pair much more easily than pure ZnO, the Ce^{4+} ion captured electrons on GCE surface and then acted as an electron trap to enhance the electron-hole pair, which further increased the catalytic performance of Ce doped ZONFs in ROSs generation. The relative reactions were showed as follows:

$$Ce^{4+} + e^- \rightarrow Ce^{3+} \quad (1)$$

$$Ce^{3+} + H_2O_2 \rightarrow Ce^{4+} + O_2^{\cdot -} \quad (2)$$

The generated $O_2^{\cdot -}$ could react with luminol, and the ECL signal of luminol was obtained. More notably, a quick $Ce^{4+} \leftrightarrow Ce^{3+}$ reaction could increase the rate of ECL reaction through the fast electron transfer and enhance the ECL intensity. As shown in Fig. 4B, the ECL peak of Ab_2-GOD@Ce:ZONFs-Lum was obtained at 5.0 s and that of Ab_2-GOD@ZONFs-Lum was observed at 5.2 s. In order to better study the ECL performance of Ab_2-GOD@ZONFs-Lum, a Potential-ECL intensity figure was

showed in Fig. S4 (Supporting Information), a higher ECL intensity and lower ECL emission potential of the Ce:ZONFs-Lum could been observed, which demonstrated ceria doped nanomaterial could increase the rate of electron transfer.

The UV-vis spectra had been exhibited in Fig. 4C and 4D. As shown in Fig. 4C, an obvious absorption (AP) peak of ZONFs was obtained at 355 nm (blue curve). And the UV-vis spectrum of Ce:ZONFs presented two AP peaks of CeO_2 at 222 nm and 317 nm (red curve), respectively, which was in accordance with the reported result[28]. Meanwhile, as shown Fig. 4D, the pure luminol had three AP peaks at 212 nm, 302 nm and 347 nm (green curve), and two AP peaks of Ce:ZONFs-Lum had been observed at 218 nm and 317 nm (pink curve). Compared with the UV-vis spectrum of luminol, the disappearance of the AP peak at 302 nm might attribute to the consumption of $-NH_2$ and the quantum size effect of Ce:ZONFs[29,30], which proved the immobilization of luminol on Ce:ZONFs surface via -NHCO-. To further prove the existence of -NHCO- in the ECL complex, the FT-IR spectrum of Ce:ZONFs-Lum was detected and showed in Fig. S5 (Supporting Information), a strong peak at 3392 cm^{-1} corresponded the N-H of secondary amide (RCONHR'), and an absorbance peak of C=O was observed at 1610-1690 cm^{-1}, which confirmed that luminol was combined onto the Ce:ZONFs by -NHCO-.

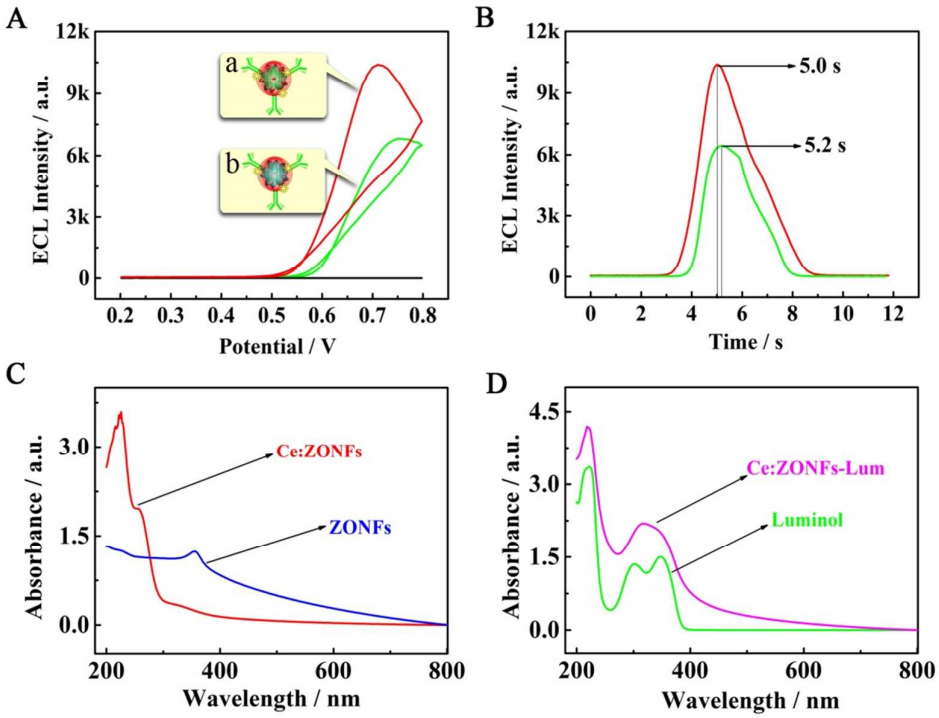

Fig. 4 (A) ECL responses of immunosensors by using different signal probes: (a) Ab_2-GOD@Ce:ZONFs-Lum probe, and (b) Ab_2-GOD@ZONFs-Lum probe. (B) The time to obtain the ECL peaks by using different signal probes: Ab_2-GOD@Ce:ZONFs-Lum probe (red curve) and Ab_2-GOD@ZONFs-Lum probe (green curve). (C) The UV-vis spectra of Ce:ZONFs and pure ZONFs. (D) The UV-vis spectra of luminol and Ce:ZONFs-Lum complex.

3.5 Detection of Aβ by the fabricated ECL immunosensor

Under the optimized experimental conditions, the ECL responses of the immunosensor with different Aβ concentrations were detected in PBS (pH 7.4, within 10 mM glucose) and were showed in Fig. 5. The ECL intensity increased with the increasing of Aβ concentration from 80 fg/mL to 100 ng/mL. And in the

inset of Fig. 5, the corresponding calibration plot was present, indicating that there was an excellent linear relationship between the intensity of ECL signals and the logarithm of Aβ concentrations. The linear equation was I = 8472.9 + 1861.4 lg c with a square of correlation coefficient was 0.9960. Additionally, a relatively low limit detection of 52 fg/mL was obtained which demonstrated the high sensitivity of the proposed biosensor. Meanwhile, we had compared our work with other methods in Aβ detection[31,32,33]. As shown in Table 1, the constructed ECL immunosensor in our work represented a wider linear range and a lower limit of detection, exhibiting its superior performance in Aβ analysis.

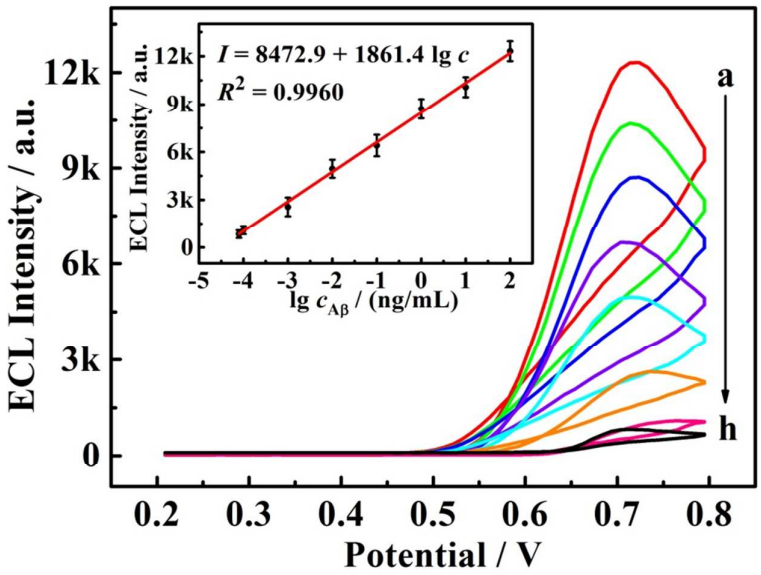

Fig. 5 ECL intensities of the proposed ECL immunosensor with different Aβ concentrations: (a) 80 fg/mL; (b) 100 fg/mL; (c) 1 pg/mL; (d) 10 pg/mL; (e) 100 pg/mL; (f) 1 ng/mL; (g) 10 ng/mL and (h) 100 ng/mL. Inset is the calibration plot of Aβ determination.

Table 1 Comparison of proposed immunosensor with other immunosensors in Aβ detection.

Measurement protocol	Linear range	Detection limit	Reference
SPR	100~2000 pg/mL	---	31
LSPR	10^{-3}~10^{5} nM	1.5 pM	32
Fluorescence	0.5~8.0 nM	0.2 nM	33
ECL	0.08~10^{5} pg/mL	52 fg/mL	Present work

3.6 Specificity, stability and reproducibility of the proposed immunosensor

In order to evaluate the specificity of the proposed ECL immunosensor, several interfering proteins including CEA and AFP were detected by the proposed immunosensor, and the results were showed in Fig. 6A. According to Fig. 6A, there was no obvious difference among the ECL signals which obtained from pure CEA, pure AFP and the blank, and the intensities of these signals were extremely low. Meanwhile, there was an ECL intensity comparison between pure Aβ (1 ng/mL) and a mixed solution (including 1 ng/mL of Aβ, 10 ng/mL of CEA and 10 ng/mL of AFP). As a result, the ECL responses were quit strong and no obvious difference between Aβ and the mixture. Therefore, the proposed immunosensor had great selectivity for Aβ. Simultaneously, Fig. 6B showed that the ECL signal intensity was directly related to the concentration of Aβ, meanwhile, these signals could prove the nice stability of proposed immunosensor. Moreover, the reproducibility of the proposed sensor was investigated by detecting the ECL signals with four different electrodes in the same conditions. As shown in Fig. 6C, four ECL signals

with four electrodes were relatively the same with a low relative standard deviation (R.S.D) of 1.86%, which meant that the immunosensor had a superior reproducibility.

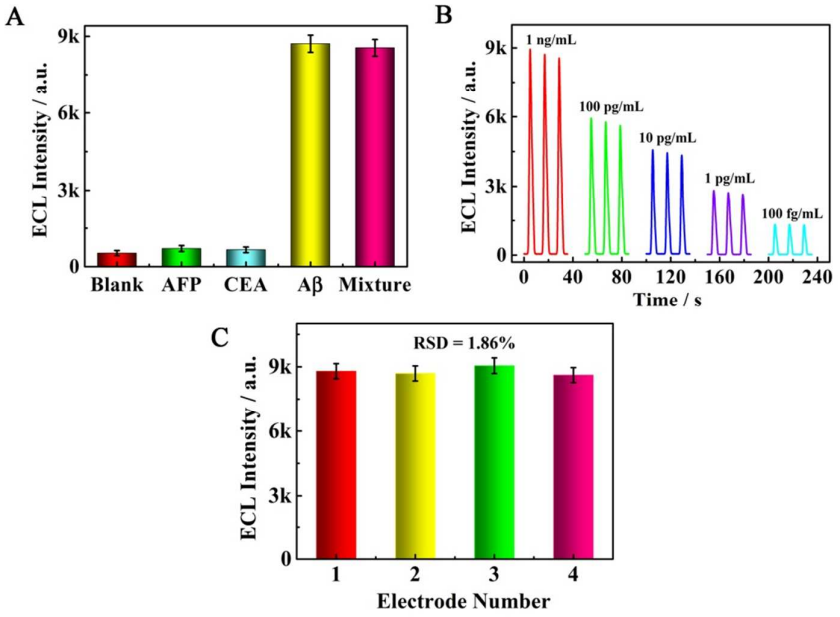

Fig. 6 (A) Selectivity of the proposed ECL immunosensor: blank, AFP (10 ng/mL), CEA (10 ng/mL), Aβ (1 ng/mL), and the Mixture (containing 10 ng/mL of AFP, 10 ng/mL of CEA and 1 ng/mL of Aβ); (B) Stability of the immunosensor with the Aβ concentration from 1 ng/mL to 100 fg/mL; (C) Reproducibility of the designed immunosensor with four electrodes, and the concentration of Aβ in this experiment was 1 ng/mL.

3.7 Application of the proposed immunosensor in real samples

To verify the promising potential of the constructed immunosensor in Alzheimer's disease detection, a recovery experiment was designed by adding varies

concentrations of Aβ into 40-fold diluted healthy human serum (the serum was supplied by Daping Hospital, Chongqing, China). Clearly seen from Fig. 7A, the red curve exhibited the ECL signal of developed immunosensor which was incubated with 1 ng/mL of Aβ (diluted with human serum), while the blue one was the signal of diluted serum only. Meanwhile, Fig. 7B is a histogram which showed a comparison of ECL intensity related to different Aβ concentrations added into different conditions (the red column represented Aβ added in PBS buffer while the green one represented Aβ added in diluted serum). As a result, the ECL intensities of the same Aβ concentration with different conditions hadn't changed too much. In addition, the recovery results were presented in Table 1. The recovery rate ranged from 89.2% to 114%, which proved that the provided immunosensor had a promising potential for Aβ determination in clinical diagnostics.

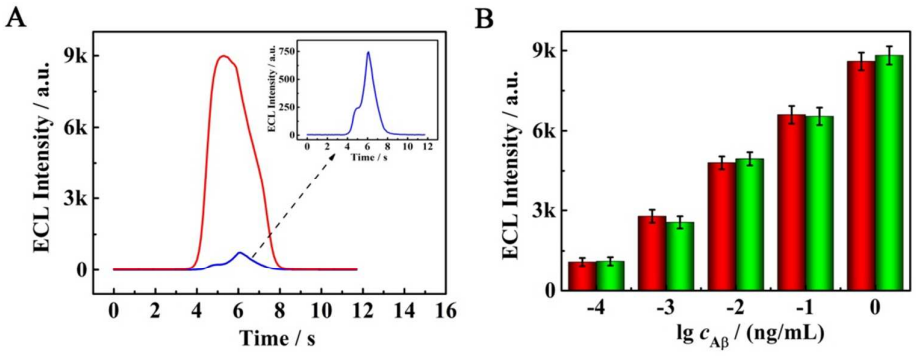

Fig. 7 (A) ECL responses of the immunosensor in 1 ng/mL Aβ added in real sample (red curve) and real sample only (blue curve). (B) Comparison of ECL responses in different Aβ concentrations and different conditions (the red column is Aβ added in PBS and the green one is Aβ added in diluted serum).

Table 2 Analytical application of the sensor in real sample

Sample number	Added/(ng/mL)	Found/(ng/mL)	Recovery/%
1	1.00	1.14	114
2	0.100	0.0913	91.3
3	0.0100	0.0106	106
4	0.00100	0.000892	89.2
5	0.000100	0.000111	111

4. Conclusion

In this work, a flower structured ceria doped ZnO nanomaterial capped with luminol was successfully synthesized and utilized to fabricate an immunosensor for Aβ detection. The prepared ECL bioconjugate, Ab_2-GOD@Ce:ZONFs-Lum, had several advantages in ECL enhancement and clinical diagnostics. Firstly, the prepared Ce:ZONFs in this work had large specific surface area, which could bind abundant of Ab_2 and the luminophore of luminol. In addition, this Ce:ZONFs had an excellent catalytic ability for H_2O_2 which served as a co-reactant of luminol, significantly enhancing the ECL signal and improving the sensitivity of the immunosensor. Lastly, a protein-like AgCys nanowire with large number of carboxyl was used as substrate for binding anti-Aβ, which could greatly improve the stability of the immunosensor. In summary, this work synthesized a novel nanomaterial Ce:ZONFs for luminol-based ECL immunosensor fabrication, providing a new method for ultrasensitive detection of protein.

ASSOCIATED CONTENT

Supporting Information The SEM image of AgCys NWs; FT-IR and UV-vis spectra of AgCys; ECL spectrum of the prepared Ab_2 bioconjugate (Ab_2@Ce:ZONFs-Lum); ECL dynamic curves of Ce:ZONFs-Lum and ZONFs-Lum; FT-IR spectrum of Ce:ZONFs-Lum.

ACKNOLEDGEMENT

This work was financially supported by the NNSF of China (21275119, 21575116, 51473136) and the Fundamental Research Funds for the Central Universities (XDJK2015A002), China.

REFERENCES

[1] Shankar, G.M.; Bloodgood, B.L.; Townsend, M.; Walsh, D.M.; Selkoe, D.J.; Sabatini, B.L. Natural Oligomers of the Alzheimer Amyloid-β Protein Induce Reversible Synapse Lose by Modulating an NMDA-Type Glutamate Receptor Dependent Signaling Pathway. *J. Neurosci.* **2007**, *27*, 2866-2875.

[2] Schutz, A.K.; Vagt, T.; Huber, M.; Ovchinnikova, O.Y.; Cadalbert, R.; Wall, J.; Guntert, P.; Bockmann, A.; Glockshuber, R.; Meier, B.H. Atomic-Resolution Three-Dimensional Structure of Amyloid β Fibrils Bearing the Osaka Mutation. *Angew. Chem. Int. Ed.* **2015**, *54*, 331-335.

[3] Blennow, K.; Leon, M.J.; Zetterberg, H. Alzheimer's Disease. *Lancet* **2006**, *368*, 387-403.

[4] Yu, Y.Y.; Zhang, L.; Li, C.L.; Sun, X.Y.; Tang, D.Q.; Shi, G.Y. A Method for Evaluating the Level of Soluble β-Amyloid$_{(1\text{-}40/1\text{-}42)}$ in Alzheimer's Disease Based on the Binding of Gelsolin to β-Amyloid Peptides. *Angew. Chem. Int. Ed.* **2014**, *53*, 12832-12835.

[5] Xu, S.J.; Liu, Y.; Wang, T.H.; Li, J.H. Positive Potential Operation of a Cathodic Electrogenerated Chemiluminescence Immunosensor Based on Luminol and Graphene for Cancer Biomarker Detection. *Anal. Chem.* **2011**, *83*, 3817-3823.

[6] Lv, X.H.; Pang, X.H.; Li, Y.Y.; Yan, T.; Cao, W.; Du, B.; Wei, Q. Electrochemiluminescent Immune-Modified Electrodes Based on Ag_2Se@CdSe Nanoneedles Loaded with Polypyrrole Intercalated Graphene for Detection of CA72-4. *ACS Appl. Mater. Interfaces* **2015**, *7*, 867-872.

[7] Habtamu, H.B.; Sentic, M.; Silvestrini, M.; De Leo, L.; Not, T.; Arbault, S.; Manojlovic, D.; Sojic, N.; Ugo, P. A Sensitive Electrochemiluminescence Immunosensor for Celiac Disease Diagnosis Based on Nanoelectrode Ensembles. *Anal. Chem.* **2015**, *87*, 12080-12087.

[8] Pang, X.H.; Li, J.X.; Zhao, Y.B.; Wu, D.; Zhang, Y.; Du, B.; Ma, H.M.; Wei, Q. Label-Free Electrochemiluminescence Immunosensor for Detection of Carcinoembryonic Antigen Based on Nanocomposites of GO/MWCNT-COOH/Au@CeO_2. *ACS Appl. Mater. Interfaces* **2015**, *7*, 19260-19267.

[9] Zhou, J.; Gan, N.; Li, T.H.; Hu, F.T.; Li, X.; Wang, L.H.; Zheng, L. A Cost-Effective Sandwich Electrochemiluminescence Immunosensor for Ultrasensitive

Detection of HIV-1 Antibody Using Magnetic Molecularly Imprinted Polymers as Capture Probes. *Biosens. Bioelectron.* **2014**, *15*, 199-206.

[10] Gu, W.L.; Deng, X.; Gu, X.X.; Jia, X.F.; Lou, B.H.; Zhang, X.W.; Li, J.; Wang, E.K. Stabilized, Superparamagnetic Functionalized Graphene/Fe_3O_4@Au Nanocomposites for a Magnetically-Controlled Solid-State Electrochemiluminescence Biosensing Application. *Anal. Chem.* **2015**, *87*, 1876-1881.

[11] Li, S.F.; Zhang, X.M.; Du, W.X.; Ni, Y.H.; Wei, X.W. Chemiluminescence Reactions of a Luminol System Catalyzed by ZnO Nanoparticles. *J. Phys. Chem. C* **2009**, *113*, 1046-1051.

[12] Sarangi, S.N.; Nozaki, S.; Sahu, S.N. ZnO Nanorod-Based Non-Enzymatic Optical Glucose Biosensor. *J. Biomed. Nanotechnol.* **2015**, *11*, 988-996.

[13] He, Y.; Yang, B.; Cheng, G. On the Oxidative Coupling of Methane with Carbon Dioxide over CeO_2/ZnO Nanocatalysts. *Catal. Today* **2004**, *98*, 595-600.

[14] Ahmed, S.M.; Szymanski, P.; El-Nadi, L.M.; El-Sayed, M.A. Energy-Transfer Efficiency in Eu-Doped ZnO Thin Films: The Effects of Oxidative Annealing on the Dynamics and the Intermediate Defect States. *ACS Appl. Mater. Interfaces* **2014**, *6*, 1765-1772.

[15] Li, X.H.; Zhang, Z.J.; Tao, L. A Novel Array of Chemiluminescence Sensors for Sensitive, Rapid and High-Throughput Detection of Explosive Triacetone Triperoxide at the Scene. *Biosens. Bioelectron.* **2013**, *47*, 356-360.

[16] Younis, A.; Chu, D.W.; Lin, X.; Yi, J.B.; Dang, F.; Li, S.A. High-Performance Nanocomposite Based Memristor with Controlled Quantum Dots as Charge Traps. *ACS Appl. Mater. Interfaces* **2013**, *5*, 2249-2254.

[17] Liu, W.; Liu, X.F.; Feng, L.J.; Guo, J.X.; Xie, A.R.; Wang, S.P.; Zhang, J.C.; Yang, Y.Z. The Synthesis of CeO_2 Nanospheres with Different Hollowness and Size Induced by Copper Doping. *Nanoscale* **2014**, *6*, 10693-10700.

[18] Tian Z.M.; Li, J.; Zhang, Z.Y.; Gao, W.; Zhou, X.M.; Qu, Y.Q. Highly Sensitive and Robust Peroxidase-like Activity of Porous Nanorods of Ceria and Their Application for Breast Cancer Detection. *Biomaterials* **2015**, *59*, 116-124.

[19] Turner, S.; Lazar, S.; Freitag, B.; Egoavil, R.; Verbeeck, J.; Put, S.; Strauven, Y.; Tendeloo, G.V. High Resolution Mapping of Surface Reduction in Ceria Nanoparticles. *Nanoscale* **2011**, *3*, 3385-3390.

[20] Truong, Q.D.; Le, T.H.; Kimura, T.; Yin, S.; Sato, T.; Ling, Y.C. Hierarchical ZnO Nanostructures: Controlling the Synthesis and Photocatalytic Decomposition of Nitrogen Monoxide. *RSC Adv.* **2013**, *3*, 19154-19160.

[21] Cheng, B.C.; Xiao, Y.H.; Wu, G.S.; Zhang, L.D. Controlled Growth and Properties of One-Dimensional ZnO Nanostructures with Ce as Activator/Dopant. *Adv. Funct. Mater.* **2004**, *14*, 913-919.

[22] Liang, X.Y.; Ren, Y.P.; Bai, S.; Zhang, N.; Dai, X.L.; Wang, X.; He, H.P.; Jin, C.H.; Ye, Z.Z.; Chen, Q.; Chen, L.W.; Wang, J.P.; Jin, Y.Z. Colloidal Indium-Doped Zinc Oxide Nanocrystals with Tunable Work Function: Rational Synthesis and Optoelectronic Applications. *Chem. Mater.* **2014**, *26*, 5169-5178.

[23] Prasanna, V.L.; Vijayaraghavan, R. Insight into the Mechanism of Antibacterial Activity of ZnO: Surface Defects Mediated Reactive Oxygen Species Even in the Dark. *Langmuir* **2015**, *31*, 9155-9162.

[24] Zheng, T.T.; Zhang, Q.F.; Feng, S.; Zhu, J.J.; Wang, Q.; Wang, H. Robust Nonenzymatic Hybrid Nanoelectrocatalysts for Signal Amplification toward Ultrasensitive Electrochemical Cytosensing. *J. Am. Chem. Soc.* **2014**, *136*, 2288-2291.

[25] Deng, C.Y.; Chen, J.H.; Nie, Z.; Wang, M.D.; Chu, X.C.; Chen, X.L.; Xiao, X.L.; Lei, C.Y.; Yao, S.Z. Impedimetric Aptasensor with Femtomolar Sensitivity Based on the Enlargement of Surface-Charged Gold Nanoparticles. *Anal. Chem.* **2009**, *81*, 739-745.

[26] Chen, W.J.; Zhang, L.Y.; Wang, M.L.; Chi, Y.W.; Chen, G.N. Preparation of Protein-like Silver-Cysteine Hybrid Nanowires and Application in Ultrasensitive Immunoassay of Cancer Biomarker. *Anal. Chem.* **2013**, *85*, 9655-9663.

[27] Jiang, X.Y.; Chai, Y.Q.; Wang, H.J.; Yuan, R. Electrochemiluminescence of Luminol Enhanced by the Synergetic Catalysis of Hemin and Silver Nanoparticles for Sensitive Protein Detection. *Biosens. Bioelectron.* **2014**, *54*, 20-26.

[28] Liu, B.W.; Sun, Z.Y.; Huang, P-J.J.; Liu, J.W. Hydrogen Peroxide Displacing DNA from Nanoceria: Mechanism and Detection of Glucose in Serum. *J. Am. Chem. Soc.* **2015**, *137*, 1290-1295.

[29] Liu, Y.; Tolentino, J.; Gibbs, M.; Ihly, R.; Perkins,C.L.; Liu, Y.; Crawford, N.; Hemminger, J.C.; Law, M. PbSe Quantum Dot Field-Effect Transistors with Air-Stable Electron Mobilities above 7 $cm^2V^{-1}s^{-1}$. *Nano Lett.* **2013**, *13*, 1578-1587.

[30] Zhou, Y.; Zhuo, Y.; Liao, N.; Chai, Y.Q.; Yuan, R. Ultrasensitive Immunoassay Based on a Pseudobienzyme Amplifying System of Choline Oxidase and Luminol-Reduced Pt@Au Hybrid Nanoflowers. *Chem. Commun.* **2014**, *50*, 14627-14630.

[31] Lee, Y.K.; Lee, K.S.; Kim, W.M.; Sohn, Y.S. Detection of Amyloid-β42 Using a Waveguide-Coupled Bimetallic Surface Plasmon Resonance Sensor Chip in the Intensity Measurement Mode. *PLOS ONE* **2014**, *9*, e98992.

[32] Kang, M.K.; Lee, J.W.; Nguyen, A.H.; Sim, S.J. Label-Free Detection of ApoE4-Mediated β-amyloid Aggregation on Signal Nanoparticle Uncovering Alzheimer's Disease. *Biosens. Bioelectron.* **2015**, *72*, 197-204.

[33] Pi, J.L.; Long, Y.J.; Huang, N.; Cheng, Y.; Zheng, H.Z. A Sandwich Immunoassay for Detection of $A\beta_{1\text{-}42}$ Based on Quantum Dots. *Talanta* **2016**, *146*, 10-15.

TOC

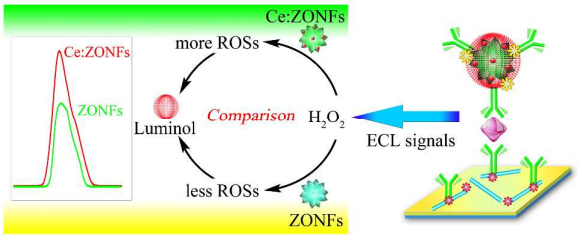
Ce:ZONFs
more ROSs
Ce:ZONFs
ZONFs
Luminol
Comparison
H_2O_2
ECL signals
less ROSs
ZONFs